



<b>Experiment title:</b> XAFS study of $\text{LaMn}_{1-x}\text{Mg}_x\text{O}_3$ perovskites: The role of disorder in mixed-valence state of Mn atom.	<b>Experiment number:</b> HS-1714	
<b>Beamline:</b> BM29	<b>Date of experiment:</b> from: 24-JUL-04 to: 30-JUL-04	<b>Date of report:</b> 22-JUL-05
<b>Shifts:</b> 8	<b>Local contact(s):</b> Gianluca Ciatto	<i>Received at ESRF:</i>

**Names and affiliations of applicants (\* indicates experimentalists):**

**G. Subías\*, J. Blasco\*, J. García\*, J. Herrero-Martín\* and M. C. Sánchez.**

*Instituto de Ciencia de Materiales de Aragón, CSIC- Universidad de Zaragoza, Departamento de Física de la Materia Condensada, C/ Pedro Cerbuna 12, 50009 Zaragoza*

## Report:

$\text{LaMn}_{1-x}\text{Mg}_x\text{O}_3$  single phases can be formed up to  $x=0.5$ . A double perovskite is observed for  $x \geq 0.4$  whereas no long Mn/Mg ordering is detected for  $x \leq 0.3$ . The electronic and geometrical local structure of Mn have been studied by means of x-ray absorption spectroscopy.

The measurements at the Mn K-edge were carried out at the BM29 beam line. A fixed-exit Si(111) double-crystal monochromator with an estimated energy resolution of  $\Delta E/E = 8 \times 10^{-5}$  was used. The absorption spectra were recorded in transmission mode at room temperature using ionization chambers as detectors. A Mn foil was simultaneously measured at room temperature for energy calibration. X-ray absorption near edge structure (XANES) spectra were normalized to the high part of the spectrum (around 100 eV above the absorption edge) after a linear background subtraction. Extended x-ray absorption fine structure (EXAFS) spectra ( $\chi(k)$ ) were obtained by removing the smooth atomic absorption coefficient ( $\mu_0$ ) by means of a cubic spline fit. The Fourier Transform (FT) of the k-weighted EXAFS spectra was calculated between 3.0 and 12.0  $\text{\AA}^{-1}$  using a Gaussian window. The EXAFS spectra were analyzed using FEFF 8.10. The structural analysis was performed in the R-space fitting mode up to 2.2  $\text{\AA}$ . The model used to fit the first shell Mn K-edge data takes into account only Mn-O single scattering paths.

Figure 1-left shows the XANES spectra of the  $\text{LaMn}_{1-x}\text{Mg}_x\text{O}_3$  samples compared to the reference compounds,  $\text{LaMnO}_3$  ( $\text{Mn}^{3+}$ ) and  $\text{CaMnO}_3$  ( $\text{Mn}^{4+}$ ). The XANES spectra for  $\text{LaMn}_{1-x}\text{Mg}_x\text{O}_3$  show a strong resonance at energies (1<sup>st</sup> inflection point) ranging between 6550.9 ( $x=0$ ) and 6554.5 eV ( $x=0.5$ ). The main difference among the spectra concerns to the position of this resonance (absorption edge). There is a continuous shift towards higher energies with increasing the Mg-content of the sample. The energy shift of the edge relative to Mn metal is collected in table 1. This shift can be correlated to the formal Mn valency. The edge for  $x \leq 0.4$  samples lies at intermediate positions between  $\text{CaMnO}_3$  and  $\text{LaMnO}_3$ , confirming a mixed valence state for the Mn atoms. The edge position for  $x=0.5$  instead is almost identical to that for  $\text{CaMnO}_3$  (see Fig. 1 left) indicating a maximum  $\text{Mn}^{4+}$  oxidation state in this sample. The XANES spectra also show broad resonances above the absorption edge, ascribed to multiple scattering effects, and weak pre-

peak resonances at  $\sim 10$  eV below the absorption edge. The pre-peak resonances show complicated structures. They are displayed in detail in the inset of Fig. 1(a) after subtracting the edge contribution.

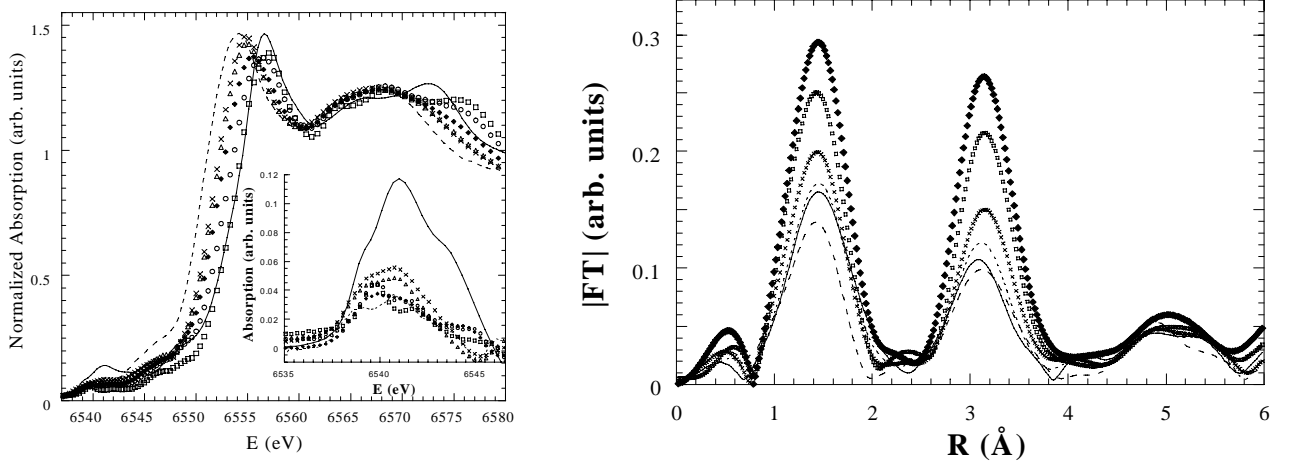


**Figure 1.** Left: Mn K-edge XANES spectra for  $\text{LaMnO}_3$  (broken line),  $\text{LaMn}_{0.9}\text{Mg}_{0.1}\text{O}_3$  (crosses),  $\text{LaMn}_{0.8}\text{Mg}_{0.2}\text{O}_3$  (triangles),  $\text{LaMn}_{0.7}\text{Mg}_{0.3}\text{O}_3$  (diamonds),  $\text{LaMn}_{0.6}\text{Mg}_{0.4}\text{O}_3$  (circles),  $\text{LaMn}_{0.5}\text{Mg}_{0.5}\text{O}_3$  (squares) and  $\text{CaMnO}_3$  (solid line). Inset: Detail of the pre-peak features after subtracting the background. Right: Fourier transform for  $\text{LaMnO}_3$  (broken line),  $\text{LaMn}_{0.9}\text{Mg}_{0.1}\text{O}_3$  (solid line),  $\text{LaMn}_{0.8}\text{Mg}_{0.2}\text{O}_3$  (dotted line),  $\text{LaMn}_{0.7}\text{Mg}_{0.3}\text{O}_3$  (crosses),  $\text{LaMn}_{0.6}\text{Mg}_{0.4}\text{O}_3$  (squares),  $\text{LaMn}_{0.5}\text{Mg}_{0.5}\text{O}_3$  (diamonds).

Figure 1-right shows the FT for the whole series compared to the undoped compound,  $\text{LaMnO}_3$ . All of the FT spectra show two strong peaks below 4 Å. The first one at around 1.5 Å (without phase-shift correction) corresponds to the first coordination shell (Mn-O). The second peak, above 3 Å, is associated to the second shell with Mn-Mg(Mn), Mn-La and Mn-O contributions together with multiple scattering paths. The intensity of both peaks increases as the content of Mg does. The increase of both peaks is in agreement with the diminution of the orthorhombic distortion in the unit cell. For instance, the first coordination shell in  $\text{LaMnO}_3$  is composed by three Mn-O distances (with a strong Jahn-Teller tetragonal distortion) whereas there is only one Mn-O distance for the rhombohedral  $\text{LaMn}_{0.5}\text{Mg}_{0.5}\text{O}_3$ . The series follows a continuous evolution between both environments. The best-fit parameters of the analysis for the first coordination shell are summarized in the table 1. An average Mn-O distance is observed for all doped samples. Such a distance decreases as the content of Mg increases in agreement with the increase of Mn valency. A minimum value of 1.89 Å is found for  $x=0.4$  and  $x=0.5$  in accordance to typical values of  $\text{Mn}^{4+}$  oxides such as  $\text{CaMnO}_3$ . On the other hand, the highest is the Mn valency the lowest is  $\sigma^2$ . This result agrees with the presence of regular  $\text{MnO}_6$  octahedra in  $x \geq 0.4$  samples.

<i>Sample</i>	$\Delta E_0$ (eV)	N	$R_{\text{Mn-O}}$ (Å)	$\sigma^2 \times 10^{-3}$ (Å <sup>2</sup> )
$\text{LaMn}_{0.5}\text{Mg}_{0.5}\text{O}_3$	16.8	6	1.89(1)	2.0(7)
$\text{LaMn}_{0.6}\text{Mg}_{0.4}\text{O}_3$	16.3	6	1.89(1)	3.9(7)
$\text{LaMn}_{0.7}\text{Mg}_{0.3}\text{O}_3$	15	6	1.90(1)	6.5(7)
$\text{LaMn}_{0.8}\text{Mg}_{0.2}\text{O}_3$	14.6	6	1.92(1)	7.9(6)
$\text{LaMn}_{0.9}\text{Mg}_{0.1}\text{O}_3$	14.6	6	1.93(1)	8.2(7)
$\text{LaMnO}_3$	13.2	4	1.92(1)	3.1(6)
		2	2.15(1)	3.5(7)

**Table 1.** Relative energy shift of the absorption edge (respect to a Mn foil as reference,  $E_0 = 6537.7$  eV) and the best fit results from the structural analysis of the first shell of the  $\text{LaMn}_{1-x}\text{Mg}_x\text{O}_3$  series at the Mn K-edge. N is the coordination number,  $R_{\text{Mn-O}}$  is the interatomic distance and  $\sigma^2$  is the Debye-Waller factor. Numbers in parentheses are statistical errors in the last significant digit.